TU München Bibliothek

SUBITO-2010062100997

subito-Normaldienst
Nutzergruppe 8

erfasst: 2010-06-21 11:16:01
fällig: 2010-06-24 11:16:01

Lieferweg: EMAIL
Format: PDF
Land: AM

Yerevan State University library
Alex Manoogyan 1

AM - 375049 Yerevan

FAX:

MAIL: elpub@ysu.am

Unter Anerkennung des Urheberrechtsgesetzes wird bestellt:

ISSN	0021-4922
Zeitschrift	Japanese journal of applied physics / 2
Aufsatz-Autor	
Aufsatz-Titel	
Band/Heft	46 / 38
Jahrgang	2007
Seiten	L923-L926
Bemerkung	

Signatur 0206 0206/Ohne Sign.

Vermerk der Bibliothek:

O	Jahrgang nicht vorhanden	O	beim Buchbinder
O	verliehen	O	vermißt
O	nicht am Standort	O	Sonstiges

Vermerk für den Kunden:
Bei Rückfragen zu Ihrem Auftrag wenden Sie sich bitte per Mail an die Dokumentlieferung subitoteam@ub.tum.de oder per Telefon unter +49 089/289-28456.

Japanese Journal of Applied Physics
Vol. 46, No. 38, 2007, pp. L923–L926

Analytical Description of Intravalley Acoustic Phonon Limited Electron Mobility in Ultrathin Si Plate Incorporating Phonon Modulation due to Plate Interfaces

Shigeyasu UNO* and Nobuya MORI[1]

Department of Electrical Engineering and Computer Science, Graduate School of Engineering, Nagoya University, Nagoya 464-8603, Japan
[1]*Department of Electronic Engineering, Graduate School of Engineering, Osaka University, Osaka 565-0871, Japan*

(Received April 16, 2007; revised July 30, 2007; accepted August 26, 2007; published online September 28, 2007)

An analytical formula for the intravalley acoustic phonon limited electron mobility in an ultrathin silicon plate is presented. Phonon modulation due to mechanical mismatch at silicon surfaces is incorporated. The resulting mobility is less than that calculated without phonon modulation, because of a form factor increase at a small in-plane phonon wave vector. An analytical expression for the form factor is proposed and used to derive explicit formulae for the intravalley acoustic phonon scattering rate and related electron mobility. The analytical mobility formula has excellent accuracy for a plate thickness less than 6 nm for 4-fold valley electrons and a plate thickness less than 3 nm for 2-fold valley electrons. [DOI: 10.1143/JJAP.46.L923]

KEYWORDS: confined acoustic phonon, FinFET, double gate, electron mobility

Acoustic phonon waves in nano scale devices are different from bulk phonons due to mechanical mismatch between different materials (e.g., Si/SiO_2, GaAs/AlAs, and GaN/AlN). Investigations on such modulated acoustic phonons and their impact on electron–phonon interactions are becoming much more important in advanced device research.[1–4] Nano-scale metal–oxide–semiconductor field-effect transistors (MOSFETs), such as silicon-on-insulator (SOI) MOSFETs, and double-gate (DG) and FinFETs, also undergo such phonon modulation effects. Preliminary calculations on scattering rates for such silicon-based devices have been carried out,[6,7] and, recently, Donetti *et al.* reported that the phonon-limited electron mobility calculated using modulated phonons is less than that obtained using bulk phonons.[8] This decrease has been observed both for a silicon plate covered with SiO_2 and a free-standing silicon plate. In ultrathin silicon plates, major electron-mobility-limiting mechanisms are intravalley acoustic phonon scattering, intervalley phonon scattering,[9] surface roughness scattering, Coulomb scattering,[10] and silicon-thickness-fluctuation-induced scattering.[11] At room temperature, phonon scattering plays an important role even with the other scattering mechanisms.[10,11] Phonon modulation affects intravalley acoustic phonon scattering only, because it is the only scattering mechanism that is mediated by long-wavelength phonons. The total electron mobility eventually decreases owing to such phonon modulation effects on the intravalley acoustic phonon scattering, even with other scattering mechanisms.[8] However, the mechanism of such mobility reduction is not yet clear. Furthermore, obtaining such modulated acoustic phonon-limited electron mobility requires complicated time-consuming numerical calculations. An in-depth study of the mobility reduction is required for a better understanding of the underlying physics, as well as to provide a simpler description of the mobility reduction, which can be used in hand calculation and device simulations. In this paper, we report an analysis of the mechanism and a simpler description of the effect of phonon modulation on electron mobility. Our analysis is focused on intravalley acoustic phonon scattering and the related electron mobility. The analysis is performed for a free-standing silicon plate for simplicity, as has been carried out for planar MOSFETs.[12]

*E-mail address: uno@nuee.nagoya-u.ac.jp

Acoustic phonon waves in an isotropic material is governed by Navier's equation:

$$\rho \frac{\partial^2 \boldsymbol{S}}{\partial t^2} = (\lambda + 2\mu)\nabla(\nabla \cdot \boldsymbol{S}) - \mu \nabla \times (\nabla \times \boldsymbol{S}), \qquad (1)$$

where $\boldsymbol{S}$ is the displacement vector, ρ is the mass density, and λ and μ are Lamé constants. The phonon wave $\boldsymbol{S}$ is expanded by normal modes as follows:

$$\boldsymbol{S}(\boldsymbol{r}, t) = \sum_{\boldsymbol{q}} C_{\boldsymbol{q}} e^{-i\omega_{\boldsymbol{q}} t} e^{i\boldsymbol{Q}\cdot\boldsymbol{R}} \boldsymbol{v}(z), \qquad (2)$$

where the three-dimensional vector $\boldsymbol{v}(z)$ represents the z dependence of the normal modes, $\omega_{\boldsymbol{q}}$ is the phonon energy, $C_{\boldsymbol{q}}$ is a constant, and $\boldsymbol{R} = (x, y)$ and $\boldsymbol{Q} = (q_x, q_y)$ are the position and phonon wave vectors in the x–y plane, respectively. Phonon wave propagation is often assumed to be along the x-axis without any loss of generality. Although q_x can take any value, the z component of the phonon wave vector, q_l, is restricted to discrete allowed values. Such discreteness of q_l leads to phonon energy dispersion branches, which can be found for silicon in the literature.[8] Using Fermi's golden rule, the transition probability for elastic acoustic deformation potential (ADP) scattering is given by

$$T(n\boldsymbol{K}, n'\boldsymbol{K}') = \frac{\pi D_{\text{aco}}^2 k_{\text{B}} T_{\text{L}}}{\hbar L_x L_y v_l^2 \rho} I_{n,n'} \delta(E_{n'} - E_n), \qquad (3)$$

where (n, n') are electron quantum numbers of confinement before/after scattering, E_n and $E_{n'}$ are electron energy as functions of in-plane electron wave vectors $\boldsymbol{K}$ and $\boldsymbol{K}'$, respectively, D_{aco} is the ADP constant, $L_x L_y$ is the plate area, k_{B} is the Boltzmann constant, T_{L} is the lattice temperature, and v_l is the longitudinal sound velocity. The quantity $I_{n,n'}$ is the form factor defined as

$$I_{n,n'}(q_x) \equiv \sum_{q_l} \frac{L_x L_y v_l^2 \rho}{\omega_{\pm q}^2} \left| \langle n' | \left\{ i q_x v_x + \frac{\partial v_z}{\partial z} \right\} | n \rangle \right|^2, \qquad (4)$$

where summation over q_l is taken for all allowed discrete values, the v_x and v_z are the x and z components of $\boldsymbol{v}(z)$, respectively. For bulk phonons, the form factor is given by

$$I_{n,n',\text{bulk}} = \frac{1}{2\pi} \int_{-\infty}^{\infty} |\langle n' | e^{iqz} | n \rangle|^2 dq, \qquad (5)$$

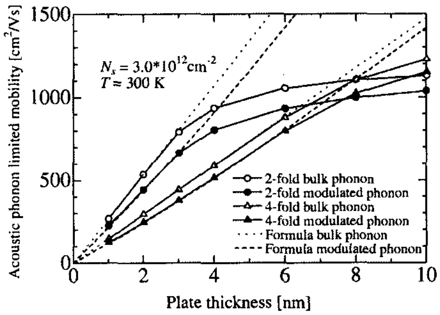

Fig. 1. Intravalley acoustic phonon-limited electron mobility as function of silicon plate thickness. Open and closed symbols: numerical results calculated using bulk and modulated phonons, respectively. Dashed and dotted curves: compact formulae, eqs. (12) and (13), with $n = 1$.

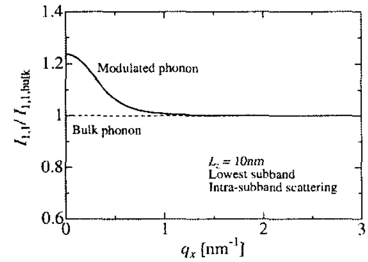

Fig. 2. Form factor for intra-lowest-subband scattering ($n = n' = 1$) numerically calculated using modulated phonons, as a function of q_x. The form factor is normalized by that calculated using bulk phonons.

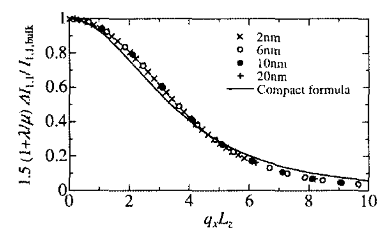

Fig. 3. Form factor increase ratio divided by right-hand side of eq. (6) plotted as function of q_xL_z. Symbols: numerical results, solid line: compact formula eq. (7).

where q is regarded as a continuous variable. With eqs. (3)–(5), acoustic phonon limited scattering rate and electron mobility are calculated with/without phonon modulation.

Figure 1 shows the numerical results of the intravalley acoustic phonon-limited electron mobility calculated for 2- and 4-fold electrons using bulk and modulated phonons, as a function of silicon plate thickness. The results are the weighted averages of electron mobility for each subband calculated with the relaxation time approximation. Material constants were determined according to the literature,[13] and $D_{\rm aco}$, m_l^*, and m_t^* were set to be 12 eV, $0.916m_0$, and $0.19m_0$, respectively. The surface electron density was set to $3.0 \times 10^{12}\,{\rm cm}^{-2}$, and the electron and lattice temperatures were both 300 K. The electron wave functions in an infinite-square-well potential were used for simplicity. In reality, for DG and FinFET, electron wave functions are modulated owing to the gates on both sides of the plate. However, they have similar shapes as the simple ones in an infinite square well when the silicon layer thickness is smaller than about 5 nm and the electric field is less than 0.1 MV/cm.[14,15] In such situations, using simple wave functions gives reasonable results. For a thicker silicon layer, a stronger vertical electric field, or single-gated SOI MOSFETs, more realistic electron wave functions may be needed for quantitative discussions. The mobility increase due to the electron occupancy increase of the 2-fold electrons[9,11,17] is not observed, because the mobility is plotted separately for 2- and 4-fold electrons. Because Fig. 1 shows the mobility limited only by intravalley acoustic phonon scattering, the mobilities for 2- and 4-fold electrons have similar values, as has been reported for a planar MOSFET inversion layer.[16] The electron mobility reduction due to phonon modulation is observed, as has been calculated using the Monte Carlo method by Donetti *et al.*[8] Our result was obtained using the relaxation time approximation, which is more convenient for an analytical description of electron mobility. Figure 2 shows a numerical result of the form factor as a function of q_x. The form factor is normalized by that calculated using bulk phonons. The calculation was carried out for intra-lowest-subband scattering ($n = n' = 1$), and the Si plate thickness was set to be 10 nm. The material parameters of silicon were taken from the literature.[13] Note that the form factor calculated using modulated phonons is larger than that obtained using bulk phonons at a small q_x, while they are equal at large q_x. The increase in the form factor directly leads to an increase in scattering rate, and hence a reduction in electron mobility. The increase at $q_x = 0$, $\Delta I_{n,n}(0) \equiv I_{n,n}(0) - I_{n,n,{\rm bulk}}$, divided by the form factor obtained using bulk phonons is exactly given by

$$\Delta I_{n,n}(0)/I_{n,n,{\rm bulk}} = 2/[3(1 + \lambda/\mu)], \qquad (6)$$

for any $n = 1, 2, \ldots$. The increase at $q_x = 0$ originates from the surface modes, which decay exponentially from the surfaces. Thus, the reduction in the electron mobility is partly due to surface phonon modes, which does not appear in bulk material. Figure 3 shows the form factor increase ratio $[I_{1,1}(q_x) - I_{1,1,{\rm bulk}}]/I_{1,1,{\rm bulk}}$ divided by the right-hand side of eq. (6), plotted as a function of q_xL_z. Symbols show numerical results obtained for different plate thicknesses. Note that all the data points lie on a universal curve regardless of plate thickness. The solid curve shows the following analytical fit for the curve:

$$\frac{3}{2}\left(1 + \frac{\lambda}{\mu}\right)\frac{\Delta I_{n,n}(q_x)}{I_{n,n,{\rm bulk}}} = \frac{4n^4\pi^2 \tanh(\xi)}{\xi(\xi^4 + 5n^2\pi^2\xi^2 + 4n^4\pi^2)}, \qquad (7)$$

where $\xi = 0.22q_xL_z$, which gives good agreement for at least $1 \le n \le 5$. Assuming isotropic scattering, the intra-subband scattering rate is written as

$$\frac{1}{\tau_{n,{\rm intra}}(E_{xy})} = n_{\rm v}\frac{D_{\rm aco}^2 m_{\rm d}^* k_{\rm B} T_L}{v_l^2 \rho \hbar^3} F_{n,n}(E_{xy}), \qquad (8)$$

where $m_{\rm d}^*$ is the density-of-state mass, $n_{\rm v}$ is the valley degeneracy. The function $F_{n,n}(E_{xy})$ is an integral of the form factor defined by

$$F_{n,n}(E_{xy}) \equiv \frac{1}{2\pi}\int_0^{2\pi} I_{n,n}\left(2\sqrt{(1-\cos\theta)E_{xy}m_{\rm c}^*/\hbar^2}\right)d\theta, \quad (9)$$

where $m_{\rm c}^*$ is the conductivity mass. By approximating $1 - \cos\theta = 1$ and using the analytical expression eq. (7), the intra-subband scattering rate is written as

$$\frac{1}{\tau_{n,\mathrm{intra}}(E_{xy})} = n_\mathrm{v}\frac{D_\mathrm{aco}^2 m_\mathrm{d}^* k_\mathrm{B} T_L}{v_l^2 \rho \hbar^3}\frac{1}{L_z}\left[\frac{3}{2} + \frac{1}{1+(\lambda/\mu)}\frac{4n^4\pi^2\tanh(\xi)}{\xi(\xi^4+5n^2\pi^2\xi^2+4n^4\pi^2)}\right], \tag{10}$$

where $\xi = 0.22 \times 2\sqrt{E_{xy} m_\mathrm{c}^*/\hbar^2} L_z$. The electron mobility is calculated as follows:

$$\mu_{n,\mathrm{intra}} = \frac{e}{m_\mathrm{c}^*}\left(\int_0^\infty \tau_{n,\mathrm{intra}}(\varepsilon k_\mathrm{B} T_\mathrm{e})\varepsilon e^{-\varepsilon} d\varepsilon \bigg/ \int_0^\infty e^{-\varepsilon} d\varepsilon\right), \tag{11}$$

where T_e is electron temperature. Using eq. (10) and assuming that the scattering rate weakly depends on ε for $\varepsilon \sim 1$, the following mobility formula is obtained:

$$\mu_{n,\mathrm{intra}} \simeq \frac{e v_l^2 \rho \hbar^3}{n_\mathrm{v} D_\mathrm{aco}^2 m_\mathrm{c}^* m_\mathrm{d}^* k_\mathrm{B} T_L}\left\{\frac{1}{L_z}\left[\frac{3}{2} + \frac{1}{1+(\lambda/\mu)}\frac{4n^4\pi^2\tanh(\xi_0)}{\xi_0(\xi_0^4+5n^2\pi^2\xi_0^2+4n^4\pi^2)}\right]\right\}^{-1}, \tag{12}$$

where $\xi_0 = 0.22 \times 2\sqrt{m_\mathrm{c}^* k_\mathrm{B} T_\mathrm{e}/\hbar^2} L_z$. For bulk phonons,

$$\mu_{n,\mathrm{bulk}} = \frac{e v_l^2 \rho \hbar^3}{n_\mathrm{v} D_\mathrm{aco}^2 m_\mathrm{c}^* m_\mathrm{d}^* k_\mathrm{B} T_L}\left(\frac{3}{2L_z}\right)^{-1}. \tag{13}$$

In Fig. 1, results from eqs. (12) and (13) with $n = 1$ are shown by dotted and dashed lines, respectively. Note that the lines obtained from the analytical formulae show excellent agreement with the numerical results for a small plate thickness. This is due to the fact that a majority of electrons are on the lowest subband for a small plate thickness, even at room temperature. The formula is valid up to 6 nm for 4-fold valley electrons, while it is valid up to 3 nm for 2-fold. The wider applicable silicon thickness range for 4-fold electrons is attributed to their lighter confinement mass, that is, larger subband energy spacing.

The above results and formulations give several implications for electron mobility in ultrathin body MOSFETs. First, the phonon-modulation-induced mobility degradation occurs at a wide range of plate thicknesses for both 2- and 4-fold electrons; thus, phonon modulation is not a major factor in choosing the best silicon thickness for the best FET performance. The numerical data in Fig. 1 indicates that the acoustic phonon mobility reduction due to phonon modulation occurs for a wide range of plate thicknesses (at least up to 10 nm). Moreover, the amount of the reduction does not strongly depend on plate thickness. Because intravalley acoustic phonon scattering plays a major role, even with intervalley and surface roughness scatterings, the phonon-modulation-induced mobility reduction lowers the total electron mobility by roughly the same ratio at a plate thickness less than 12 nm.[8] These facts indicate that the phonon modulation does not affect the optimum plate thickness for the best FET performance. Reducing silicon thickness markedly improves the subthreshold slope,[18] but at the cost of electron mobility degradation.[11,17] It has also been shown experimentally for SOI MOSFETs that a plate thickness of approximately 3.4 nm gives the advantage of phonon-limited mobility enhancement, even with silicon-thickness-fluctuation-induced scattering.[11] Optimum silicon thickness might therefore be approximately 3.4 nm. According to eq. (12), the experimental mobility at that plate thickness contains a phonon-modulation-induced degradation of about 15%. Although the existence of SiO_2 and intervalley scattering weakens this estimation, phonon-modulation-induced degradation might still be effective to some extent. Second, the acoustic phonon-limited electron mobility reduction due to phonon modulation might be more significant in Ge channels. Equations (6) and (12) indicate that $\eta \equiv 1/[1+(\lambda/\mu)]$ is a good indicator for the significance of the acoustic phonon-limited mobility reduction due to phonon modulation; the larger this value is, the more significant the mobility reduction will be. The η values for Si, Ge, and GaAs are 0.355, 0.541, and 0.528, respectively. This indicates that using alternative channel materials such as Ge or GaAs might result in a stronger phonon modulation. This will not be an issue for GaAs, because the major scattering mechanism is polar optical phonon scattering. However, for Ge, the merit of high electron mobility may be weakened by phonon-modulation-induced electron mobility degradation. A quantitative evaluation requires a more accurate modeling such as an analysis of inter-subband scattering, the incorporation of surrounding materials such as SiO_2, and the incorporation of gate-modulated electron wave functions.

In summary, the modulated acoustic phonon-limited electron mobility in an ultrathin silicon plate has been analyzed. The electron mobility reduction attributes to the form factor increase at a small in-plane phonon wave vector owing partly to surface modes. The explicit analytical formula for the form factor has been presented. This formula has been used to derive compact models for the intravalley acoustic phonon-limited electron mobility, which achieves excellent accuracy for a silicon plate thickness less than 6 nm for 4-fold valley electrons and a silicon plate thickness less than 3 nm for 2-fold valley electrons.

We would like to thank Professor Yong of Harvey Mudd College for mathematical advice. This research was partially supported by a Grant-in-Aid for Young Scientists (B) (No. 18760251, 2006) from the Ministry of Education, Culture, Sports, Science and Technology, Japan.

1) N. Bannov, V. Aristov, V. Mitin, and M. A. Stroscio: Phys. Rev. B **51** (1995) 9930.
2) S. M. Komirenko, K. W. Kim, A. A. Demidenko, V. A. Kochelap, and M. A. Stroscio: Phys. Rev. B **62** (2000) 7459.
3) B. A. Glavin, V. I. Pipa, V. V. Mitin, and M. A. Stroscio: Phys. Rev. B **65** (2002) 205315.
4) E. P. Pokatilov, D. L. Nika, and A. A. Balandin: Appl. Phys. Lett. **85** (2004) 825.
5) E. P. Pokatilov, D. L. Nika, and A. A. Balandin: J. Appl. Phys. **95** (2004) 5626.
6) S. Uno and N. Mori: Proc. Device Research Conf., 2005, p. 226.
7) S. Uno and N. Mori: Proc. Solid State Devices and Materials, 2005, p. 430.
8) L. Donetti, F. Gámiz, J. B. Roldán, and A. Godoy: J. Appl. Phys. **100** (2006) 13701.
9) S. Takagi, J. Koga, and A. Toriumi: Jpn. J. Appl. Phys. **37** (1998) 1289.

10) F. Gámiz, J. López-Villanueva, J. Roldán, J. Carceller, and P. Cartujo: IEEE Trans. Electron Devices **45** (1998) 1122.
11) K. Uchida, H. Watanabe, A. Kinoshita, J. Koga, T. Numata, and S. Takagi: IEDM Tech. Dig., 2002, p. 47.
12) H. Ezawa: Ann. Phys. (N.Y.) **67** (1971) 438.
13) M. V. Fischetti: IEEE Trans. Electron Devices **38** (1991) 634.
14) B. Majkusiak, T. Janik, and J. Walczak: IEEE Trans. Electron Devices **45** (1998) 1127.
15) M. Shoji and S. Horiguchi: J. Appl. Phys. **85** (1999) 2722.
16) S. Takagi, J. Hoyt, J. Welser, and J. Gibbons: J. Appl. Phys. **80** (1996) 1567.
17) D. Esseni, A. Abramo, L. Selmi, and E. Sangiorgi: IEEE Trans. Electron Devices **50** (2003) 2445.
18) J. Park and J. Colinge: IEEE Trans. Electron Devices **49** (2002) 2222.